# Kapitza resistance and the thermal conductivity of amorphous superlattices

Ashutosh Giri, Patrick E. Hopkins, James G. Wessel, and John C. Duda

Citation: Journal of Applied Physics **118**, 165303 (2015); doi: 10.1063/1.4934511
View online: http://dx.doi.org/10.1063/1.4934511
View Table of Contents: http://scitation.aip.org/content/aip/journal/jap/118/16?ver=pdfcov
Published by the AIP Publishing

# Kapitza resistance and the thermal conductivity of amorphous superlattices

Ashutosh Giri,[1] Patrick E. Hopkins,[1] James G. Wessel,[2] and John C. Duda[2,a)]
[1]*Department of Mechanical and Aerospace Engineering, University of Virginia, Charlottesville, Virginia 22904, USA*
[2]*Seagate Technology, Bloomington, Minnesota 55435, USA*

(Received 21 July 2015; accepted 10 October 2015; published online 23 October 2015)

We report on the thermal conductivities of amorphous Stillinger-Weber and Lennard-Jones superlattices as determined by non-equilibrium molecular dynamics simulations. Thermal conductivities decrease with increasing interface density, demonstrating that interfaces contribute a non-negligible thermal resistance. Interestingly, Kapitza resistances at interfaces between amorphous materials are lower than those at interfaces between the corresponding crystalline materials. We find that Kapitza resistances within the Stillinger-Webber based Si/Ge amorphous superlattices are not a function of interface density, counter to what has been observed in crystalline superlattices. Furthermore, the widely used thermal circuit model is able to correctly predict the interfacial resistance within the Stillinger-Weber based amorphous superlattices. However, we show that the applicability of this widely used thermal circuit model is invalid for Lennard-Jones based amorphous superlattices, suggesting that the assumptions made in the model do not hold for these systems.  [http://dx.doi.org/10.1063/1.4934511]

## I. INTRODUCTION

The electrical and optical properties of amorphous semiconductor superlattices (SLs) have been a subject of scientific inquiry since Abeles and Tiedje first provided evidence that the SLs exhibit quantum size effects.[1] In addition, amorphous SLs provided a platform for some of the earliest experimental observations of the coherent characteristics of lattice vibrations,[2] including the formation of zone-folded acoustic modes[3] and phonon stop bands.[4] These vibrational modes in amorphous and disordered solids have been described using a different taxonomy compared to crystalline materials due to the lack of periodicity in their atomic arrangement.[5] Unlike in crystalline solids, vibrations in amorphous and disordered materials are classified as propagons (that are delocalized, propagating modes), diffusons (that are non-propagating, delocalized modes) and locons (that are localized and non-propagating modes).[6] While locons do not contribute to the thermal conductivity, diffusions mediate heat through harmonic coupling of localized modes.[7,8]

In amorphous SLs, even though the propagating low frequency vibrations are affected by the artificial periodicity due to their extensive coherence lengths, it is generally assumed that the amorphicity within each layer should dictate the properties of higher frequency, non-propagating vibrations (and hence, thermal transport).[9] Under this assumption, interfaces within amorphous SLs would not provide any additional thermal resistance. This perspective was supported by the report of Zhang *et al.*[10] where the measured thermal diffusivities of a-Si:H/a-$SiN_x$:H SLs were well described by effective medium theory when the interfaces within the SLs were ignored.

Interfaces between dissimilar crystals readily scatter phonons due to differences in stiffness, density, and structure.[11,12] As a result, crystalline SLs exhibit thermal conductivities lower than those of their constituent components when the distance between consecutive interfaces is less than the phonon mean-free-paths intrinsic to either material.[13–25] This approach to thermal conductivity reduction has proven particularly successful in Si-based material systems where heat carrying phonons have mean-free-paths as long as several micrometers.[26–28] On the other hand, thermal transport in amorphous materials can be largely mediated diffusons.[29–32] Once again, this conceptual description is consistent with the experimental observations referenced above. In turn, interfaces are not generally regarded as major contributors to thermal resistance in amorphous material systems.

In this report, we implement non-equilibrium molecular dynamics (NEMD) simulations to study the role of Kapitza resistance on the vibrational thermal transport in amorphous SLs. We asses the roles of varying vibrational length scales on thermal resistances in these amorphous SLs by concomitantly simulating thermal transport using both Stillinger-Weber (SW) and Lennard-Jones (LJ) interatomic potentials. We find that interfaces begin to non-negligibly contribute to the thermal resistivity of amorphous SLs at interface densities $\geq 0.1\,\mathrm{nm}^{-1}$. These interface densities are a factor of two higher than those considered in previous reports,[10] explaining the discrepancies between these findings. From our thermal conductivity data, we calculate the effective Kapitza resistances at interfaces within the SLs by applying the widely used thermal circuit model. The Kapitza resistance increases as the vibrational mismatch between the constituent materials increases (as it does in crystalline SLs). However, we note that the Kapitza resistance at an amorphous interface is lower than at a corresponding crystalline interface for both SW- and LJ-based solids. This observation provides evidence that interfacial thermal transport is primarily mediated by diffusons in these SLs. Furthermore, the

a)Electronic mail: duda@seagate.com

 

Kapitza resistance does not appear to be a function of interface density for the SW-based SLs, contrary to what has been found for their corresponding crystalline SLs. Additionally, when comparing our results using SW potentials to those assuming LJ potentials, we find that he thermal circuit model cannot correctly predict the Kapitza resistances for the amorphous LJ-based SLs, demonstrating the insufficiencies of this widely used model in predicting thermal transport in LJ-based SLs.

## II. METHODOLOGY

The thermal conductivities of amorphous semiconductor multilayers and the Kapitza resistances at interfaces between amorphous thin films were calculated via NEMD simulations using the LAMMPS molecular dynamics package.[33] We created our "silicon-like" computational domains by starting with a single species of atoms arranged along a diamond cubic lattice with a lattice constant of 5.44 Å; two domain lengths were considered to check for finite size effects, $d = 125$ Å and 250 Å. Interatomic interactions were specified by the SW potential parameterized for Si (Ref. 34), Ge (Ref. 35), and Si-Ge (Ref. 36). A time step of 1 fs was used throughout the duration of the simulations, and periodic boundary conditions were initially applied in the x-, y-, and z-directions during equilibration and later altered during NEMD. The crystals were heated from 0 K to above the melt temperature via a velocity scaling routine. They were then allowed to equilibrate by imposing a NVE integration (which is the microcanonical ensemble with the number of particles, volume and total energy of the system held constant) for $1 \times 10^5$ time steps followed by NPT integration (which is the isothermal-isobaric ensemble with the number of particles, pressure and temperature of the system held constant) at zero-pressure and 2500 K for another $1 \times 10^5$ time steps. Next, the crystals were rapidly quenched to near 0 K by applying a large damping force to all atoms (with a damping coefficient of 0.031 eV ps$^{-1}$). Note, using a quench rate of $10^{12}$ K s$^{-1}$ produced statistically invariant thermal conductivities for these amorphous SLs. The distributions of atomic coordination numbers and atomic density were calculated to ensure no voids formed during solidification. We then varied atomic mass depending on the position of the atoms in the computational cells in order to create mass-mismatched SLs, an example of which is shown in Fig. 1(a).

To compare the role of interatomic potentials, we compared our SW-based systems with amorphous SLs using a different potential in the form of 6–12 LJ potential. Thermal properties of atomic structures simulated with a LJ potential can be dominated by anharmonic effects more-so than our SW structures that are defined by a 3-body interaction potential. The form of the potential is given as, $U(r) = 4\varepsilon[(\sigma/r)^{12} - (\sigma/r)^6]$, where $r$ is the interatomic separation and $\sigma$ and $\varepsilon$ are the LJ length and energy parameters. The alternating layers (i.e., A/B) in the SLs are defined by the energy and length parameter for LJ argon ($\varepsilon_{Ar} = 0.0103$ eV and $\sigma_{Ar} = 3.405$ Å, respectively),[37] and the mass-mismatch for these SLs is set to $m_A/m_B = 3$.

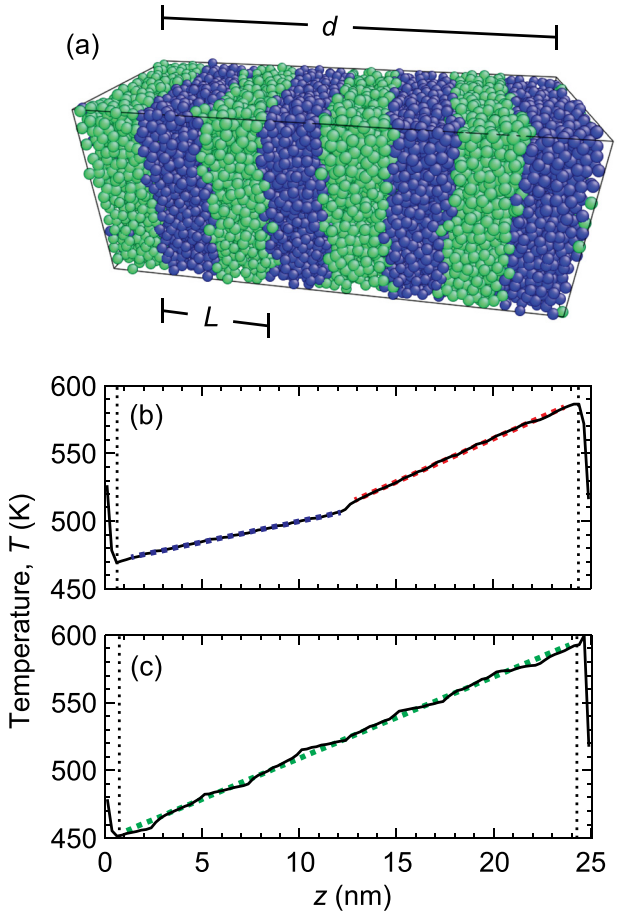


FIG. 1. (a) Schematic of a $50 \times 50 \times 125$ Å$^3$ computational domain with $N = 0.64$ nm$^{-1}$ for a SW-based SL where shading represents atomic species. Below are examples of time-averaged steady-state temperature profiles of (b) an isolated interface and (c) an amorphous multilayer with $N = 0.40$ nm$^{-1}$ for SW-based systems. The fact that the layer thicknesses in the SLs are below the regime where propagating modes affect the thermal conductivities, we observe constant temperature gradients for the layers in all of the SW-based SLs, suggesting that diffusons are the primary heat carrying vibrations in these SLs. Both temperature profiles in (b) and (c) are from simulations with a mass mismatch $m_B/m_A = 4$. The discontinuity in (b) allows for the direct calculation of Kapitza resistance at an isolated interface.

To determine thermal conductivity of the SLs and Kapitza resistance of isolated interfaces, we implemented the NEMD method. A standard steady-state NEMD simulation can be set up to investigate either the thermal conductivity of a material, $k$, or the Kapitza resistance at the interface between two different materials, $R_K$. In either case, a thermal flux, $Q$, is applied across a computational domain in order to establish a steady-state spatial temperature gradient, $\partial T/\partial x$. If the thermal conductivity is sought, the observed spatial temperature gradient can be related to the thermal conductivity by invoking the Fourier law, $Q = -k\partial T/\partial x$. As for Kapitza resistance, a temperature discontinuity at an interface, $\Delta T$, is related to conductance through the relationship $Q = R_K^{-1}\Delta T$.

Starting with an amorphous SL near 0 K, the desired simulation temperature and zero-pressure were set by performing NPT integration for $5 \times 10^5$ time-steps followed by NVT integration for $5 \times 10^5$ time-steps. A steady-state temperature gradient was then established by creating a fixed

wall separating the ends of the domain in the z-direction and performing NVE integration while adding a fixed amount of energy per time step to a warm bath at one end of the domain and removing the same amount of energy from a cool bath at the other end of the domain. Depending on the length and overall thermal resistivity of the computational domain for the SW based SLs, energy was added and removed at a rate between 0.5 and 1 eV $ps^{-1}$. The corresponding thermal flux led to a total temperature drop of ~100 K across the length of the domain for these structures. It took ~500 ps to reach steady state, at which point data were averaged for 2000 ps to create a time-averaged, steady-state temperature profile from which thermal conductivity or Kapitza resistance could be calculated. Examples of these temperature profiles are shown in Figs. 1(b) and 1(c). Similar NEMD procedure was applied to impose linear temperature gradients in the amorphous LJ multilayers. Note, decreasing the steady heat flux drastically (by ~50%) produced statistically invariant thermal conductivities calculated from the temperature profiles for a specific sample.

## III. RESULTS AND DISCUSSION

The thermal conductivities of amorphous SW Si, Ge, and Si/Ge SLs were calculated using two different domain lengths, $d = 125$ Å and 250 Å. Generally speaking, domain length can have a significant influence on the thermal conductivities predicted by NEMD simulations due to the fact that the fixed ends of the domain serve as phonon scattering sites, thereby shortening mean-free-paths and reducing observed thermal conductivities.[27,38,39] However, we do not observe any statistically significant change in the predicted thermal conductivities of amorphous Si nor of our amorphous SLs (see comparison in Fig. 2). While this may seem obvious, it is important to note that recent work in Refs. 31 and 8 have illustrated that a significant portion of the vibrations in amorphous SW Si are propagating delocalized modes (propagons). However, our period and sample thicknesses for the multilayers are not in a regime where a significant portion of the heat is carried by these propagating vibrational modes. This alludes to the fact that the majority of heat carrying vibrations can be described as diffusons in the SW-based SLs studied in this work (i.e., amorphous SW systems with thicknesses less than 250 Å). Similarly, size effects have also been reported for crystalline LJ SLs where it was shown that extrapolation methods have to be applied to correctly predict the thermal conductivities.[40,41] As with the SW-based SLs, our simulations with two domain sizes (160 Å and 220 Å) for the amorphous LJ-based multilayers produce statistically invariant thermal conductivities suggesting that no size effects are prevalent for these samples either.

The thermal conductivities of amorphous Si/Ge SLs are plotted as a function of period length, $L$, and interface density, $N$, in Figs. 2(a) and 2(b), respectively. As shown in the figure, the thermal conductivity of an amorphous Si/Ge SL increases with increasing $L$ and decreases linearly with increasing $N$. These data demonstrate that interfaces contribute a non-negligible thermal resistance. We determine the

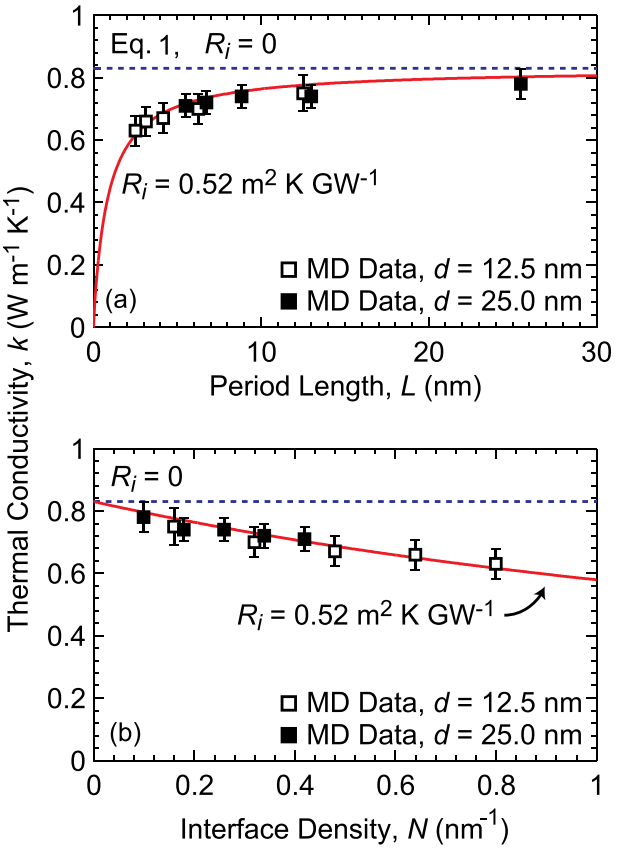


FIG. 2. Thermal conductivities of amorphous Si/Ge superlattices plotted as a function of (a) period length and (b) interface density. Hollow symbols are data from simulations with domains 125 Å long, and solid symbols are data from simulations with domains 250 Å long. The overlap of hollow and solid symbols indicates size effects did not distort our results. Also plotted is the thermal conductivity predicted by Eq. (1) when interfaces are ignored (dashed line), as well as with the best-fit value of Kapitza resistance $R_i = 0.52$ m$^2$ K GW$^{-1}$ (solid line). These results are for Si/Ge SLs in which the layers are defined by the same interaction parameters in the potential but differ in their mass ($m_A/m_B = 2.6$).

Kapitza resistance at an a:Si/a:Ge interface by applying the widely used thermal circuit model, which treats the thermal resistivity of a SL, $\rho$, as a superposition of the thermal resistances of the individual layers and the Kapitza resistances at the interfaces. That is,

$$\rho = k^{-1} = \frac{1}{L}\left[\frac{L}{2k_A} + \frac{L}{2k_B} + 2R_K\right], \tag{1}$$

where $k_A$ and $k_B$ are the thermal conductivities of the constituent components as determined from separate simulations of amorphous Si or Ge. The NEMD-predicted thermal conductivities of amorphous Si and Ge (with a domain length of 25 nm and a cross-sectional area of 24 nm$^2$) are $1.09 \pm 0.14$ W m$^{-1}$ K$^{-1}$ and $0.67 \pm 0.06$ W m$^{-1}$ K$^{-1}$, respectively. We note that for the period thicknesses considered in this work, the thermal conductivities of the amorphous materials in each layer in the SW-based SLs are statistically invariant from the thermal conductivities predicted for our "bulk" structures (i.e., $k_A$ and $k_B$ are size independent for these period thicknesses). Our NEMD-predicted thermal conductivity for amorphous Si is consistent with the Allen-Feldman theory[5] ($k = 1.2 \pm 0.1$ W m$^{-1}$ K$^{-1}$) and is

also consistent with the thermal conductivity predicted via normal mode decomposition analysis of amorphous Si that only considers the contribution from non-propagating modes as discussed in Ref. 8. However, as mentioned earlier, size effects can drastically increase the thermal conductivity of amorphous Si for large simulation domains where the significant amount of heat is carried by propagons.[8,42] In Ref. 42, NEMD results on domain lengths smaller than ~33 nm did not show a noticeable size dependence in the predicted thermal conductivity as non-propagating modes do not contribute significantly to thermal transport on this length scale. This is consistent with the results of our NEMD simulations where we do not observe any size effects in thermal conductivities for the domain lengths and layer thicknesses used for our SW-based SLs, further validating the use of thickness independent thermal conductivities as input parameters in Eq. (1) for these SLs.

Using Eq. (1), our thermal conductivity data, and a least squares fitting routine, we find that the Kapitza resistance at an a:Si/a:Ge interface is 0.52 $m^2$ K $GW^{-1}$. The thermal conductivities predicted from the least squares fitting routing are within 4% of the values determined by our NEMD simulations, demonstrating that the model fits the MD data very well. The best-fit value of Kapitza resistance is consistent with that calculated from separate NEMD simulations of isolated interfaces between amorphous Si and Ge (corresponding to temperature profiles similar to that illustrated in Fig. 1(b)). More specifically, we expect a temperature drop of 3.6 K from the Kapitza resistance predicted by Eq. (1) at the amorphous Si/heavy-Si interface shown in Fig. 1(b). From Fig. 1(c), we observe a temperature drop ~4 K at the isolated interface, which is in excellent agreement with the prediction from the thermal circuit model, suggesting that the Kapitza resistance predicted by Eq. (1) can be used to describe the internal Kapitza resistances in these SW-based amorphous SLs.

Two aspects of these data are worth noting. First, the resistance at an a:Si/a:Ge interface is ~6 times lower than at the corresponding isolated interface between crystalline Si and Ge (as determined via our additional simulations on an isolated crystalline Si/Ge interface and further verified by a previous work that studied the Kapitza resistance at isolated crystalline Si/Ge interfaces[43]). More specifically, from our additional simulations on an isolated crystalline Si/Ge interface, we find that the Kapitza resistance is 2.81 $m^2$ K $GW^{-1}$ at this interface; we note that for this crystalline Si/Ge simulation, the species differ only in mass and we conduct the simulations using a similar domain size as studied for our amorphous structures at 500 K. Our result on the mass-mismatched crystalline interface is within 5% of the MD prediction from Landry and Mcgaughey ($R_K = 2.93$ $m^2$ K $GW^{-1}$) for a crystalline Si/Ge interface.[43] The small discrepancy between the predicted Kapitza resistances might be due to the fact that our simulations do not consider the strain associated with the lattice mismatch between Si and Ge, whereas, the MD simulations in Ref. 43 consider the lattice mismatch between the species and also take into account the different interaction parameters between the species. Moreover, the fact that our domain size for the crystalline Si/Ge structure is well below the mean free path of heat carrying phonons in these structures, size effects can significantly influence the predicted Kapitza resistances across crystalline Si/Ge interfaces as shown in the work of Landry and Mcgaughey.[43] For a comprehensive study of Kapitza resistance at crystalline Si/Ge and Si/heavy-Si interfaces, the reader is referred to Ref. 43 where the authors compare their MD and lattice dynamics results to theoretical calculations.

The difference in the Kapitza resistances between amorphous and crystalline Si/Ge interfaces is despite the fact that the vibrational mismatch between amorphous Si and Ge is very similar to that between crystalline Si and Ge (see Fig. 3). While the vibrational bandwidths of these two materials are similar regardless of amorphicity or crystallinity, the vibrations that predominately contribute to thermal transport in our amorphous Si and Ge layers in the SLs are non-propagating modes. That is, the heat carrying vibrations in our amorphous Si/Ge SLs are not spatially extended as in the case of crystalline Si/Ge systems. (This conclusion can be drawn due to the absence of size effects in the context of the former and the prevalence of size effects in the context of the latter.) This is supported by our simulations on LJ-based samples as well, where we do not observe any size effects as mentioned above.

The second and related aspect worth noting is that Kapitza resistances at the interfaces within our amorphous SW SLs do not appear to be a function of interface density. On the contrary, Kapitza resistance has been shown to decrease with increasing interface density in crystalline SLs.[19,20] This behavior has been ascribed to a transition from diffusive to ballistic phonon transport, i.e., a shortening of phonon mean-free-paths.[20] Taking these two observations together, it follows that interfacial thermal transport is mediated by delocalized and non-propagating modes (or diffusons) in

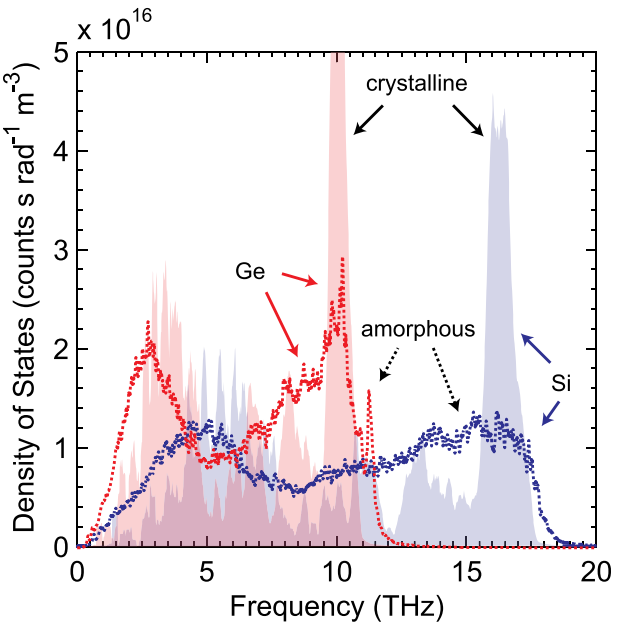


FIG. 3. Vibrational density of states of amorphous (dashed lines) and crystalline (shaded regions) Si and Ge. Regardless of amorphicity or crystallinity, the differences between the vibrational spectra between Si and Ge are similar.

these amorphous SLs. In other words, recent works have shown that the thermal boundary conductance (TBC; $R_K^{-1}$) across interfaces in SLs can increase when the SL period is less than the phonon mean free path[20] suggesting that long wavelength phonons contribute to TBC differently than short wavelength phonons; we do not observe this trend in our simulations for the Si/Ge or Si/heavy-Si SLs, which indicates that TBC in these amorphous SLs is mediated by diffusons.

The thermal conductivities of amorphous Si/heavy-Si SLs with $m_A = 28$ amu, $d = 250$ Å and $N = 0.4\,\text{nm}^{-1}$ are plotted as a function of mass-mismatch (i.e., as a function of $m_B/m_A$) in Fig. 4(a). As is evident in the plot, the thermal conductivities of amorphous SLs decrease with increasing mass-mismatch. Part of the observed reduction in thermal conductivity is due to the fact that the thermal conductivity of material B decreases as its atomic mass increases, while part of it is also due to the increasing Kapitza resistance at the interfaces between the layers as mass-mismatch increases. To gain a better understanding of the relative contributions of $k_B$ and $R_K$ to the total resistivity of the SLs, we executed a series of simulations as a function of interface density, although now for a mass-mismatch of $m_B/m_A = 4$. The best fit of Eq. (1) to these data yields $R_K = 1.04$ m$^2$ K GW$^{-1}$. With knowledge of the thermal conductivities of the SLs, the thermal conductivities of the constituent components, and the Kapitza resistances, we can determine the relative roles of $k_B$ and $R_K$ in the observed reduction in thermal conductivity as mass-mismatch increases from 2.6 to 4. For example, for a fixed interface density of $N = 0.4\,\text{nm}^{-1}$ approximately 11% of the reduction in thermal conductivity is due to increasing Kapitza resistance, while the rest is due to the lower thermal conductivity of material B.

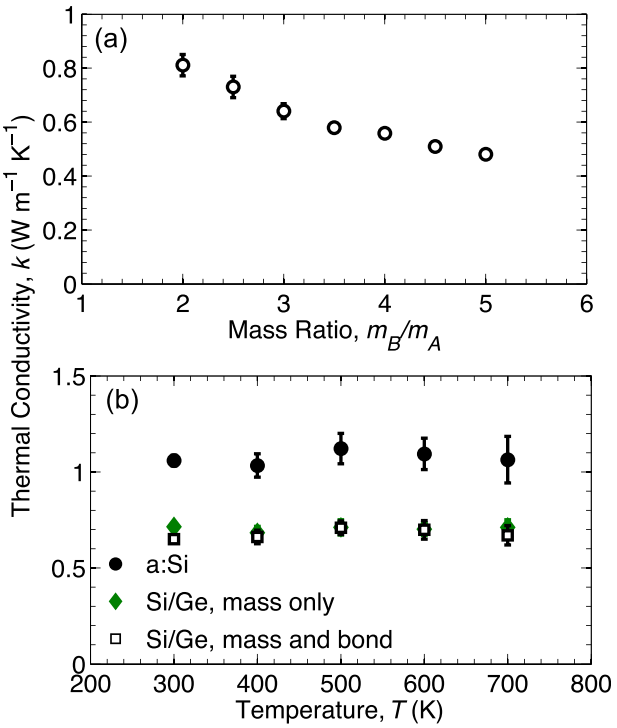


FIG. 4. (a) Thermal conductivity of amorphous Si/heavy-Si superlattices with $N = 0.4\,\text{nm}^{-1}$ as a function of mass mismatch; thermal conductivity decreases with increasing mass mismatch. Part of this reduction is due to the lower thermal conductivity of one of the materials comprising the superlattice, while the other part of the reduction is due to the increasing Kapitza resistance with increasing mass mismatch. (b) Thermal conductivity of amorphous Si and an amorphous Si/Ge superlattice as a function of temperature; no temperature dependence is observed.

The thermal conductivities of amorphous Si and two amorphous Si/Ge superlattices each with $m_A/m_B = 2.6$, $d = 250$ Å, and $N = 0.4\,\text{nm}^{-1}$ are plotted as a function of temperature in Fig. 4(b). The amorphous Si/Ge superlattices differ from each other with regard to the description of Si-Ge and Ge-Ge bonds. One superlattice is only mass-mismatched consistent with the description above, while the other also considers differences in the Si-Si, Si-Ge, and Ge-Ge bonds.[35,36] As is evident in the plot, the thermal conductivities of all systems do not exhibit a temperature dependence, contrary to purely crystalline or crystalline/amorphous SLs.[19,20,44] This suggests that anharmonic interactions are negligible in these SW-based amorphous SL structures. We caution that as our Si/Ge SLs were prepared starting from a homogeneous amorphous material, our results could potentially be different in comparison to SLs prepared using different interaction parameters for the Si/Ge species.

We conduct additional NEMD simulations on amorphous SLs defined by the LJ potential (that accounts for the general anharmonic nature of real materials). As mentioned above, we create these SLs by starting from an amorphous LJ argon and separating the layers according to the position in the structure. Our NEMD simulations on homogeneous amorphous LJ argon predict a thermal conductivity of $0.177 \pm 0.009$ W m$^{-1}$ K$^{-1}$. This is in good agreement with the Green Kubo-predicted thermal conductivity ($k = 0.180$ W m$^{-1}$ K$^{-1}$ at 10 K) for amorphous LJ argon in Ref. 45. Note, we only investigate our LJ-based SLs at low temperatures as the amorphous phase is only stable up to a temperature of ~20 K for LJ argon.[45]

Fig. 5 shows the thermal conductivity as a function of interface density for the LJ-based SLs. Similar to the SW SLs, the thermal conductivity decreases monotonically with increasing interface density for these samples. However, in contrast to the SW SLs, the Kapitza resistances predicted by fitting the MD data with Eq. (1) do not agree with the values

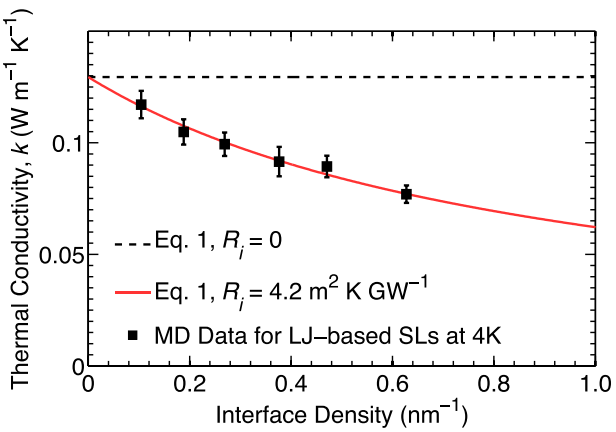


FIG. 5. Thermal conductivity of amorphous LJ SLs plotted as a function of interface density. Also shown is the thermal conductivity predicted by Eq. (1) when interfaces are ignored (dashed line), as well as the best-fit value of the Kapitza resistance (solid line).

obtained from simulations on the corresponding isolated interfaces. More specifically, simulations on an isolated interface for layers A/B predict $R_K = 13.8 \pm 1.0$ m$^2$ K GW$^{-1}$, which is higher than the value predicted by the least squares best-fit of Eq. (1) to the MD data (see Fig. 5). This disagreement suggests that the assumptions made while predicting the interfacial resistance via Eq. (1) are not valid for these LJ-based amorphous SLs. Specifically, the assumption of a constant interface resistance and the assumption that the thermal conductivities of the constituent layers being equal to that of the bulk could be invalid. This is consistent with the findings in Ref. 46, where it is demonstrated that the thermal circuit model underpredicts the thermal conductance of LJ-based crystalline SL junctions that are confined between two leads.

## IV. CONCLUSIONS

We have investigated the contribution of Kapitza resistance to the overall thermal resistivity of amorphous SW Si/Ge SLs, SW Si/heavy-Si SLs, and amorphous LJ SLs. While the Kapitza resistance at an interface between amorphous Si and Ge is smaller than that between crystalline Si and Ge, it is non-negligible when interface density approaches 0.1 nm$^{-1}$ or greater. Increasing mass-mismatch in amorphous SLs yields higher Kapitza resistances, indicating that a mismatch in vibrational spectra is responsible for the additional thermal resistance. A discussion of our data in the context of previous studies of the thermal conductivity of crystalline SLs suggests that interfacial thermal transport is predominantly mediated by delocalized non-propagating vibrational modes for amorphous Si/Ge and Si/heavy-Si SLs. Lastly, the energy exchange in these SW SLs is mostly harmonic in nature. Furthermore, the Kapitza resistance predicted from the thermal circuit model is shown to not depend on the interfacial density in these SLs. However, when considering amorphous SLs defined by an anharmonic potential such as the LJ potential, the thermal circuit model fails to replicate the Kapitza resistance at interfaces in the LJ-based SLs.


[1]B. Abeles and T. Tiedje, Phys. Rev. Lett. **51**, 2003 (1983).
[2]N. Maley and J. S. Lannin, Phys. Rev. B **31**, 5577 (1985).
[3]P. Santos, M. Hundhausen, and L. Ley, Phys. Rev. B **33**, 1516 (1986).
[4]O. Koblinger, J. Mebert, E. Dittrich, S. Döttinger, W. Eisenmenger, P. V. Santos, and L. Ley, Phys. Rev. B **35**, 9372 (1987).
[5]P. B. Allen and J. L. Feldman, Phys. Rev. B **48**, 12581 (1993).
[6]P. B. Allen, J. L. Feldman, J. Fabian, and F. Wooten, Philos. Mag. B **79**, 1715 (1999).
[7]J. L. Feldman, M. D. Kluge, P. B. Allen, and F. Wooten, Phys. Rev. B **48**, 12589 (1993).
[8]J. M. Larkin and A. J. H. McGaughey, Phys. Rev. B **89**, 144303 (2014).
[9]P. Santos and L. Ley, Superlattices Microstruct. **5**, 43 (1989).
[10]Z. Zhang, J. Roger, D. Fournier, A. Boccara, and J. Wang, Thin Solid Films **186**, 361 (1990).
[11]E. T. Swartz and R. O. Pohl, Rev. Mod. Phys. **61**, 605 (1989).
[12]P. E. Hopkins, ISRN Mech. Eng. **2013**, 682586.
[13]S.-M. Lee, D. G. Cahill, and R. Venkatasubramanian, Appl. Phys. Lett. **70**, 2957 (1997).
[14]W. S. Capinski, H. J. Maris, T. Ruf, M. Cardona, K. Ploog, and D. S. Katzer, Phys. Rev. B **59**, 8105 (1999).
[15]T. Borca-Tasciuc, W. Liu, J. Liu, T. Zeng, D. W. Song, C. D. Moore, G. Chen, K. L. Wang, M. S. Goorsky, T. Radetic, R. Gronsky, T. Koga, and M. S. Dresselhaus, Superlattices Microstruct. **28**, 199 (2000).
[16]M. N. Touzelbaev, P. Zhou, R. Venkatasubramanian, and K. E. Goodson, J. Appl. Phys. **90**, 763 (2001).
[17]S. T. Huxtable, A. R. Abramson, C.-L. Tien, A. Majumdar, C. LaBounty, X. Fan, G. Zeng, J. E. Bowers, A. Shakouri, and E. T. Croke, Appl. Phys. Lett. **80**, 1737 (2002).
[18]S. Chakraborty, C. A. Kleint, A. Heinrich, C. M. Schneider, J. Schumann, M. Falke, and S. Teichert, Appl. Phys. Lett. **83**, 4184 (2003).
[19]E. S. Landry and A. J. H. McGaughey, Phys. Rev. B **79**, 075316 (2009).
[20]Y. K. Koh, Y. Cao, D. G. Cahill, and D. Jena, Adv. Funct. Mater. **19**, 610 (2009).
[21]Y. Wang, C. Liebig, X. Xu, and R. Venkatasubramanian, Appl. Phys. Lett. **97**, 083103 (2010).
[22]Y. Chalopin, K. Esfarjani, A. Henry, S. Volz, and G. Chen, Phys. Rev. B **85**, 195302 (2012).
[23]M. N. Luckyanova, J. Garg, K. Esfarjani, A. Jandl, M. T. Bulsara, A. J. Schmidt, A. J. Minnich, S. Chen, M. S. Dresselhaus, Z. Ren, E. A. Fitzgerald, and G. Chen, Science **338**, 936 (2012).
[24]J. Ravichandran, A. K. Yadav, R. Cheaito, P. B. Rossen, A. Soukiassian, S. J. Suresha, J. C. Duda, B. M. Foley, C.-H. Lee, Y. Zhu, A. W. Lichtenberger, J. E. Moore, D. A. Muller, D. G. Schlom, P. E. Hopkins, A. Majumdar, R. Ramesh, and M. A. Zurbuchen, Nat. Mater. **13**, 168 (2014).
[25]R. M. Costescu, D. G. Cahill, F. H. Fabreguette, Z. A. Sechrist, and S. M. George, Science **303**, 989 (2004).
[26]A. S. Henry and G. Chen, J. Comput. Theor. Nanosci. **5**, 141 (2008).
[27]D. P. Sellan, E. S. Landry, J. E. Turney, A. J. H. McGaughey, and C. H. Amon, Phys. Rev. B **81**, 214305 (2010).
[28]D. P. Sellan, J. E. Turney, A. J. H. McGaughey, and C. H. Amon, J. Appl. Phys. **108**, 113524 (2010).
[29]A. Einstein, Ann. Phys. **340**, 898 (1911).
[30]D. G. Cahill, S. K. Watson, and R. O. Pohl, Phys. Rev. B **46**, 6131 (1992).
[31]S. Shenogin, A. Bodapati, P. Keblinski, and A. J. H. McGaughey, J. Appl. Phys. **105**, 034906 (2009).
[32]D. G. Cahill and R. O. Pohl, Phys. Rev. B **35**, 4067 (1987).
[33]S. Plimpton, J. Comput. Phys. **117**, 1 (1995).
[34]F. H. Stillinger and T. A. Weber, Phys. Rev. B **31**, 5262 (1985).
[35]K. Ding and H. C. Andersen, Phys. Rev. B **34**, 6987 (1986).
[36]M. Laradji, D. P. Landau, and B. Dünweg, Phys. Rev. B **51**, 4894 (1995).
[37]D. V. Matyushov and R. Schmid, J. Chem. Phys. **104**, 8627 (1996).
[38]P. K. Schelling, S. R. Phillpot, and P. Keblinski, Phys. Rev. B **65**, 144306 (2002).
[39]R. E. Jones, J. C. Duda, X. W. Zhou, C. J. Kimmer, and P. E. Hopkins, Appl. Phys. Lett. **102**, 183119 (2013).
[40]E. S. Landry, M. I. Hussein, and A. J. H. McGaughey, Phys. Rev. B **77**, 184302 (2008).
[41]Y. Chen, D. Li, J. R. Lukes, Z. Ni, and M. Chen, Phys. Rev. B **72**, 174302 (2005).
[42]Y. He, D. Donadio, and G. Galli, Appl. Phys. Lett. **98**, 144101 (2011).
[43]E. S. Landry and A. J. H. McGaughey, Phys. Rev. B **80**, 165304 (2009).
[44]A. France-Lanord, S. Merabia, T. Albaret, D. Lacroix, and K. Termentzidis, J. Phys.: Condens. Matter **26**, 355801 (2014).
[45]A. McGaughey and M. Kaviany, Int. J. Heat Mass Transfer **47**, 1783 (2004).
[46]S. Lu and A. J. H. McGaughey, AIP Adv. **5**, 053205 (2015).